Coarsening of Unstable Surface Features during Fe(001) Homoepitaxy

Joseph A. Stroscio, D. T. Pierce, M. D. Stiles, A. Zangwill[†]

Electron Physics Group
National Institute of Standards and Technology
Gaithersburg, Maryland 20899

L. M. Sander

Department of Physics, University of Michigan
Ann Arbor, MI 48109

Abstract

The evolution of the surface profile during homoepitaxial growth of Fe(001) is studied by scanning tunnelling microscopy and reflection high energy electron diffraction. The observed morphology exhibits a non-self affine collection of mound-like features that maintain their shape but coarsen as growth proceeds. The characteristic feature separation L is set in the submonolayer regime and increases with thickness, t, as $L(t) \sim t^{0.16 \pm 0.04}$. During the coarsening phase, the mounds are characterized by a magic slope and a lack of reflection symmetry. These observations are shown to be described by a continuum growth equation without capillarity.

PACS: 68.55.Jk,61.16.Ch,05.70.Ln

The basic mechanisms of epitaxial growth onto flat single crystal surfaces have been known for over fifty years[1]. In the absence of surface defects, growth occurs by the nucleation, growth, and coalescence of two-dimensional (single atom height) islands. Atoms from an external beam arrive at the surface, transfer the heat of condensation to the substrate, and begin activated surface diffusion. Pairs of migrating atoms collide randomly over the surface and may bind to form dimers. The dimers may or may not dissociate thermally before other atoms diffuse to join them. Eventually, stable nuclei form that grow in size as other atoms arrive and attach. Individual island growth continues until nearby islands begin to impinge upon one another and coalesce. Layer completion occurs as freshly deposited particles fill in the gaps between coalesced islands. In principle, this scenario repeats for each layer so that the surface roughness varies periodically in time. But in fact, shot noise in the deposition flux randomly induces nucleation of new stable nuclei on top of existing islands before layer completion occurs. The progressive roughening of the growth front implied by this picture has been the subject of numerous experimental and theoretical studies in recent years [2,3]. Part of the impetus for many of these studies has been the theoretical expectation [4] that noise-induced roughening during crystal growth might lead to self-affine surfaces [5].

Very recently however, experimental data obtained from GaAs(001) [6], Cu(001) [7], Ge(001) [8], and Pt(111) [9] has revealed that a completely different morphological scenario can occur for homoepitaxy onto high quality single crystal surfaces. The surface morphology here takes the form of a collection of fairly regular three dimensional mounds characterized by a well-defined separation distance $L(t)$. The mere existence of the single scale length $L(t)$ implies that these surfaces are not self-affine. According to Villain [10], the origin of this behavior can traced to an intrinsic instability of the flat surface that occurs in the island nucleation and coalescence regime whenever energy barriers to the transport of diffusing atoms downward over step edges exceed the usual surface diffusion barrier on a flat terrace. Since atoms on an incomplete layer that recoil from these barriers

are more likely to encounter one another, the probability for the nucleation of daughter islands onto incomplete parent islands (as sketched above) is enhanced. Repeated application of this idea in successive layers leads to a wedding-cake island structure. Quantitatively, recent theoretical work [11,12] predicts that the characteristic length scale $L(t)$ increases as $t^{1/4}$ due to capillary-induced coalescence events that eliminate smaller mounds in favor of larger mounds. As coalescence occurs, the island size distribution coarsens, i.e. the distribution becomes more dominated by larger islands at the expense of smaller islands.

As a test of these ideas, we report a scanning tunnelling microscopy (STM) and reflection-high-energy-electron diffraction (RHEED) study of the homoepitaxial growth of Fe(001) at room temperature. For all thicknesses we observe a collection of mound-like features with a characteristic separation. For thin layers, we find that the separation between mounds is the original island spacing set in the sub-monolayer regime. On subsequent growth, we show that the characteristic separation increases (coarsens) with power-law behavior, $L(t) \sim t^{0.16 \pm 0.04}$ [13]. A theoretical model without capillarity is proposed that well describes these findings. The experiments were performed in an ultra-high vacuum system with facilities for thin film growth and measurements of the surface evolution by STM and RHEED, as described previously [2]. The Fe films described in this study were all grown at substrate temperatures of 20 ^{o}C.

The typical surface morphology observed in homoepitaxial growth of Fe at 20 ^{o}C consists of a mosaic of mounds, as shown in Fig. 1(a) for a 10 monolayer film. The mound configuration develops in the earliest stages of growth and continues through multilayer growth up the maximum thickness investigated of 600 monolayers. The mound spacing is initially equal to the separation of two-dimensional islands observed at submonolayer coverages originally studied by the two of us [2,14], *i.e. the nucleated islands in the earliest stages of growth form a template for the multilayer growth stage due to the step edge barrier for diffusion.* An additional characteristic of the surface morphology in Fig. 1(a) is the

absence of reflection symmetry in the plane defined by the mean height. This is clearly seen in the contour plot shown in Fig. 1(b) where channels are observed to run through the collection of mounds.

To quantify the mound characteristics we examine the height-height correlation function, $\langle h(\mathbf{r})h(0)\rangle$, where $h(\mathbf{r})$ is the height relative to the mean height, obtained from the STM images and shown in Fig. 2. We characterize the average mound height by the root-mean-square value of the height fluctuations, $\langle h(0)h(0)\rangle^{1/2}$, and define the mound separation, $L = 2r_c$, where r_c is the position of the first zero crossing of $\langle h(\mathbf{r})h(0)\rangle$. From Fig. 2 we observe both an increase in the mound height with increasing thickness and an increase in the mound spacing. The mound separation, *L*, is shown in Fig. 3 as a function of thickness. For thickness less than ~ 3-5 monolayers the separation is equal to the initial nucleated island separation. The feature separation increases slowly as the film thickness increases. By contrast, the slope that the mounds make with respect to the surface plane rapidly *saturates* to a “magic” slope as growth proceeds (see Fig. 3). A measure of this slope is given by the ratio of mound height to lateral size, $\langle h(0)h(0)\rangle^{1/2}/r_c$, and is shown in Fig. 3. The saturated value corresponds to angle of $13 \pm 3°$, as determined from the peaks in histograms of the slopes measured by STM.

A second independent observation of a characteristic separation of mound-like features in the surface morphology is seen in RHEED measurements of the (0,0) diffraction profile where a splitting of the diffraction peak into two satellite peaks is observed [2] (inset to Fig. 2). The decrease in the peak splitting of the satellite peaks with increased layer thickness is evidence for coarsening of the mound features. The mound separation, defined as $4\pi/\Delta$, where Δ is the peak splitting, is shown as a function of thickness in Fig. 3. We find that $4\pi/\Delta$ from the RHEED measurements and $2r_c$ from the correlation functions agree as measures of the characteristic mound separation. Using these two data sets, we obtain a coarsening exponent of 0.16 ± 0.04 [13]from a linear least squares fit to

the logarithm of the feature separation against the logarithm of the thickness for thickness ≥ 20 monolayers and ≤ 600 monolayers.

We performed a numerical study of a phenomenological, continuum equation of motion to help interpret our experimental results. This approach has the great virtue that it focuses attention on general thermodynamic and kinetic features of the problem rather than on atomistic details that distinguish one material from another [10]. In the absence of desorption and void formation in the bulk, the surface height profile $h(\mathbf{r}, t)$ satisfies a continuity equation,

$$\frac{\partial h}{\partial t} = -\nabla \cdot \mathbf{j}, \tag{1}$$

that involves a mass current parallel to the surface. The deposition rate does not appear because h is the height relative to the mean height. For the present problem, we suggest that the appropriate current is the surface current,

$$\mathbf{j} = -B\nabla\nabla^2(\nabla \cdot \mathbf{m}) + \alpha\mathbf{m} - \beta m^2\mathbf{m} + \sigma\nabla(m^2) \ , \tag{2}$$

where $\mathbf{m} = \nabla h$ is the local surface slope. Before identifying each term, we remark that Eq. (2) is notable mostly for a term that is *absent*. This is the near-equilibrium current $\mathbf{j} = D\nabla(\nabla \cdot \mathbf{m})$ that was identified many years ago by Mullins [15] as arising from capillary-induced surface smoothening by surface diffusion. This term is invariably present in equations of motion intended to describe epitaxial growth [6,9,11,12,16]. But it cannot be present here because the previously established [14] absence of thermal detachment of atoms from step edges of Fe(001) at T=20 ^{o}C implies that local equilibrium cannot be established between diffusing atoms and the growing solid.

The second term in Eq. (2) is a destabilizing, mound inducing, uphill current that was shown by Villain [10] to be present whenever energy barriers inhibit the downward transport of atoms over step edges relative to surface diffusion on a flat terrace. Recent Monte Carlo simulations of our present data determine the step edge diffusion barrier on

Fe(001) [17]. The third term in Eq. (2), essentially introduced by Siegert and Plischke [12], saturates the rapid increase in local slope induced by the αm term to the value $m = \sqrt{\alpha/(3\beta)}$. This we identify as the magic slope. The microscopic origin of this term is unclear (Refs. [11] and [12] discuss some candidate mechanisms) but our data clearly speaks for the presence of a term with its properties.

Several authors have noted that the lack of up-down reflection symmetry we observe arises from a basic asymmetry in the equations of step propagation for terraces at the top of mounds as compared to terraces at the bottom of mounds [9,11,18,19]. The last term in Eq. (2) is merely the simplest one that qualitatively reproduces this effect. This brings us finally to the first term in the surface current above. Such a term has been derived from a local "corner" free energy in connection with facet growth [20]. But all thermodynamic driving forces seem to be absent from the present problem. Instead, we believe an entirely kinetic origin must be sought for this term which we justify here simply as the lowest order linear term (beyond the absent capillary term) that will induce coarsening and preserve $\mathbf{r} \rightarrow -\mathbf{r}$ symmetry. A satisfactory physical derivation remains a challenge for the future.

Numerical integration of Eq. (1) with Eq. (2) beginning with a random surface yields a collection of mound structures that compare quite favorably with the experimental data (Fig. 1(c)). We note that this agreement (as well as similar agreement with fine details of the experimental correlation functions) is destroyed if the final, symmetry-breaking term in Eq. (2) is omitted. As shown in Figure 3(b), the mounds both exhibit a magic slope and coarsen as a power law in time with an exponent 0.18 ± 0.02 , very similar to that seen in the experiment. We find that this exponent is insensitive to the presence or absence of the symmetry-breaking term. Moreover, we have verified that $t^{1/4}$ coarsening occurs if our leading term in Eq. (2) is replaced by $\mathbf{j} = D\nabla(\nabla \cdot \mathbf{m})$ [11,12] so that a crossover from $\sim t^{1/6}$ to $\sim t^{1/4}$ is expected when bond breaking due to increased temperature or strain becomes important. This connects our results to those of He et al. [21] and Thürmer

et al. [22] who observed $t^{1/4}$ coarsening for *heteroepitaxial* Fe/Au(001) and Fe/Mg(001) respectively.

The authors thank Robert Celotta and Martin Siegert for helpful correspondence and discussions. This work was supported by the Office of Technology Administration of the Department of Commerce and the Office of Naval Research. LMS is supported by NSF grant DMR 94-20335.

References

† Permanent address: School of Physics, Georgia Institute of Technology, Atlanta, Georgia, 30332.

[1] [M. Volmer, Kinetik der Phasenbildung (Steinkopff, Dresden, 1939). For a modern discussion, see J.D. Weeks and G.H. Gilmer, Adv. Chem. Phys. **40**, 157 (1979).

[2] J.A. Stroscio, D.T. Pierce, and R.A. Dragoset, Phys. Rev. Lett. **70**, 3615 (1993).

[3] see for example, S. L. Dudarev, D. D. Vvedensky and M. J. Whelan, Phys. Rev. B 50, 14525 (1994); D. E. Wolf in *Scale Invariance, Interfaces, and Non-Equilibrium Dynamics*, edited by M. Droz, A. J. McKane, J. Vannimenus, and D. E. Wolf (Plenum, New York, 1994).

[4] F. Family and T. Vicsek, eds. Dynamics of Fractal Surfaces (World Scientific, Singapore, 1991).

[5] A self affine surface profile $h(x, t)$ is statistically equivalent to the surface profile $\lambda^{-\alpha} h(\lambda x, \lambda^z t)$, where λ is a scaling factor and α and z are independent exponents.

[6] C. Orme, M.D. Johnson, J.L. Sudijono, K.T. Leung and B.G. Orr, Appl. Phys. Lett. **64**, 860 (1994); M.D. Johnson, C. Orme, A.W. Hunt, D. Graff, J.L. Sudijono, L.M. Sander and B.G. Orr, Phys. Rev. Lett. **72**, 116 (1994); G. W. Smith, A. J. Pidduck, C. R. Whitehouse, J. L. Glasper, A. M. Keir, and C. Pickering, Appl. Phys. Lett. **59**, 3282 (1991); E. J. Heller and M. G. Lagally, Appl. Phys. Lett. **60**, 2675 (1992).

[7] H.-J. Ernst, E. Fabre, R. Folkerts and J.L. Lapujoulade, Phys. Rev. Lett. **72**, 112 (1994); H.-J. Ernst, E. Fabre, R. Folkerts and J.L. Lapujoulade, J. Vac. Sci. Tech. A **12**, 1 (1994).

[8] J.E. Van Nostrand, S.J. Chey, M.-A. Hasan, D.G. Cahilll and J.E. Greene, Phys. Rev. Lett. **74**, 1127 (1995).

[9] R. Kunkel, B. Poelsema, L. K. Verheij, and G. Comsa, Phys. Rev. Lett. **65**, 733 (1990); M. Bott, T. Michely, and G. Comsa, Surf. Sci. **272**, 161 (1992).

[10] J. Villain, J. Phys. I France **1**, 19 (1991); I. Elkinani and J. Villain, J. Phys. I France **4**, 949 (1994).

[11] A. W. Hunt, C. Orme, D.R.M. Williams, B.G. Orr and L.M. Sander, Europhys. Lett. **27**, 611 (1994); A. W. Hunt, C. Orme, D.R.M. Williams, B.G. Orr and L.M. Sander in *Scale Invariance, Interfaces and Non-Equilibrium Dynamics*, edited by A.J. McKane (Plenum,New York, 1994).

[12] M. Siegert and M. Plischke, Phys. Rev. Lett. **73**, 1517 (1994); M. Siegert in *Scale Invariance, Interfaces and Non-Equilibrium Dynamics*, edited by A.J. McKane (Plenum,New York, 1994).

[13] Unless otherwise noted, all uncertainties are two standard deviations.

[14] J.A. Stroscio and D.T. Pierce, Phys. Rev. B **49**, 8522 (1994).

[15] W. W. Mullins, J. Appl. Phys. **28**, 333 (1957).

[16] See, for example, S. Das Sarma, Fractals, **1**, 410 (1994).

[17] M. C. Bartelt and J. W. Evans, Phys. Rev. Lett. **75**, 000 (Nov. 13th issue) (1995); J. G. Amar and F. Family (to be published).

[18] Z.-W. Lai and S. Das Sarma, Phys. Rev. Lett. **66**, 2348 (1991).

[19] D.D. Vvedensky, A. Zangwill, C.N. Luse and M.R. Wilby, Phys. Rev. E **48**, 852 (1993).

[20] J. Stewart and N. Goldenfeld, Phys. Rev. A **46**, 6505 (1992). F. Liu and H. Metiu, Phys. Rev. B **48**, 5808 (1993).

[21] Y.-L. He, H.-N. Yang, T.-M. Lu, and G.-C. Wang, Phys. Rev. Lett. **69**, 3770 (1992).

[22] K. Thürmer, R. Koch, M. Weber, K. H. Rieder, Phys. Rev. Lett. **75**, 1767 (1995).

Figures

Figure 1. (a) STM image of 10 monolayers of Fe grown on an Fe whisker at 20^{o} C. The image is 100 x 100 nm and the grey scale covers a range of 0.9 nm where white indicates higher portions of the surface. Note the pattern formation of mounds. (b) Contour map of a smaller 20 x 20 nm region from the left bottom corner in (a). Solid lines denote equi-height contours with the heavy line at the mean height. (c) Contour plots of the calculated surface height during growth. The parameters for the current, Eq. (2), are $B = 1.0$, $\alpha = 2.0$, $\beta = 72.0$ and $\sigma = 20.0$. The numerical integrations are done on 64×64 lattices with $\Delta x = \Delta y = 1.0$. The initial conditions are randomly chosen for each site from a Gaussian distribution of width 0.01. The surface shown is at thickness, $t = 56.23$.

Figure 2. Circularly averaged height-height correlation function versus distance obtained from STM topographic images of Fe films grown on Fe whiskers at 20^{o} C for thicknesses of (a) 2.9; (b) 5.3; (c) 20.5; and (d) 134.6 monolayers. The inset shows the RHEED profile through the (0,0) diffraction rod versus momentum transfer for film thicknesses of (a) 5.3; (b) 20.5; (c) 50.7; (d) 101.4; and (e) 134.6 monolayers.

Figure 3. (a) Feature separation and ratio of RMS height to feature separation versus film thickness. Left axis; feature separation, *L*, obtained from; (squares) $2\,r_c$, where r_c is the 1st zero crossing of the height-height correlation function, and (diamonds) $4\pi/\Delta$, where Δ is the splitting of the RHEED diffraction peaks obtained from the profiles in the inset in Fig. 2. The solid line is the result of a least-square-fit to the STM and RHEED data points for thicknesses ≥20 monolayers yielding a slope of 0.16 ± 0.04. The dashed line is the island separation observed at 0.07 monolayer coverage [14]. Right axis; a measure of the angle which the mounds make with the surface plane estimated by taking the mound height as $\langle h(0)h(0)\rangle^{1/2}$ and the lateral extent of the mound as r_c. Fe evaporation rates were ~1.5 ML/min (open symbols) and ~30 ML/min (filled symbols). (b) Feature

separation and ratio of RMS height to feature separation from numerical solution of the continuum equations. The feature separation and slope are derived from height-height correlation functions as in (a). Parameters of the integrations are as in Fig. 1(c). Each point is an average of 9 realizations. The solid line shows the least squares fit to the results for thicknesses > 150 yielding a slope of 0.18 ± 0.02.

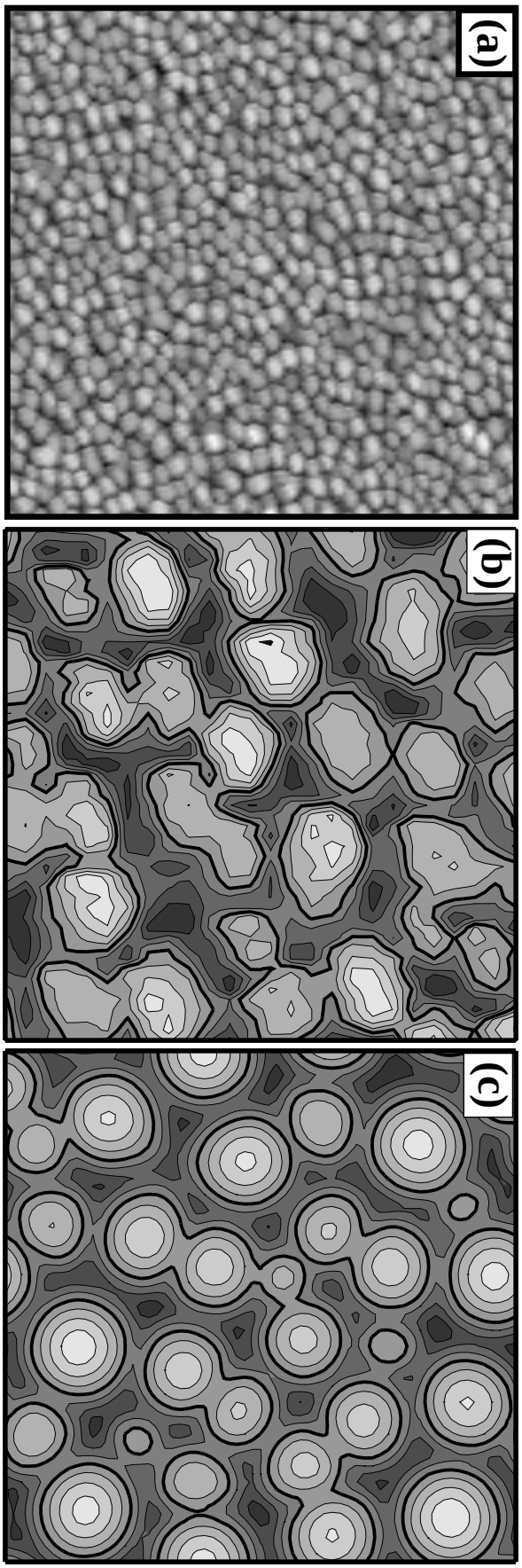

Figure 1

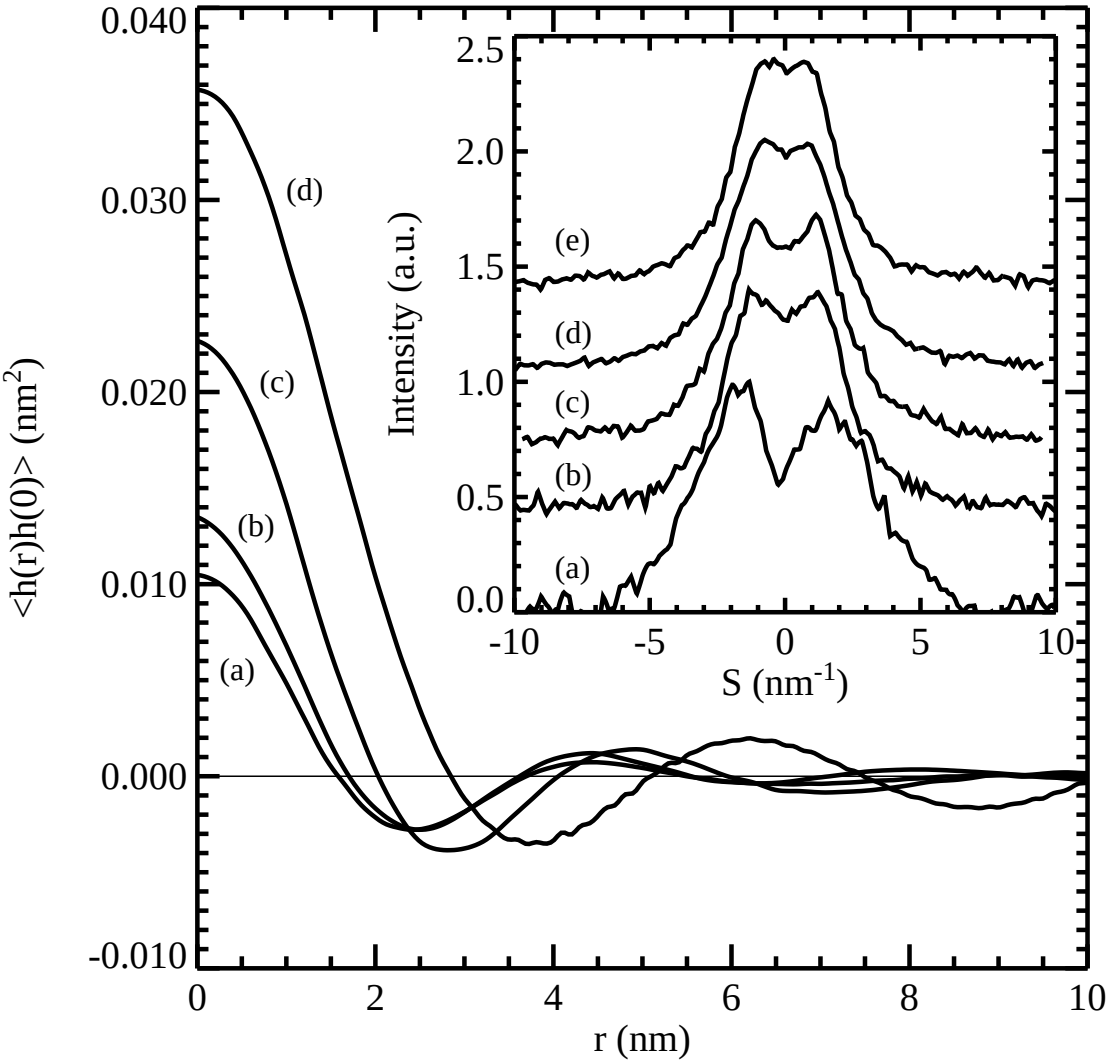
0.040
0.030
0.020
0.010
0.000
-0.010
<h(r)h(0)> (nm^2)
(d)
(c)
(b)
(a)
0
2
4
6
8
10
r (nm)
2.5
2.0
1.5
1.0
0.5
0.0
Intensity (a.u.)
(e)
(d)
(c)
(b)
(a)
-10
-5
0
5
10
S (nm^{-1})

Figure 2

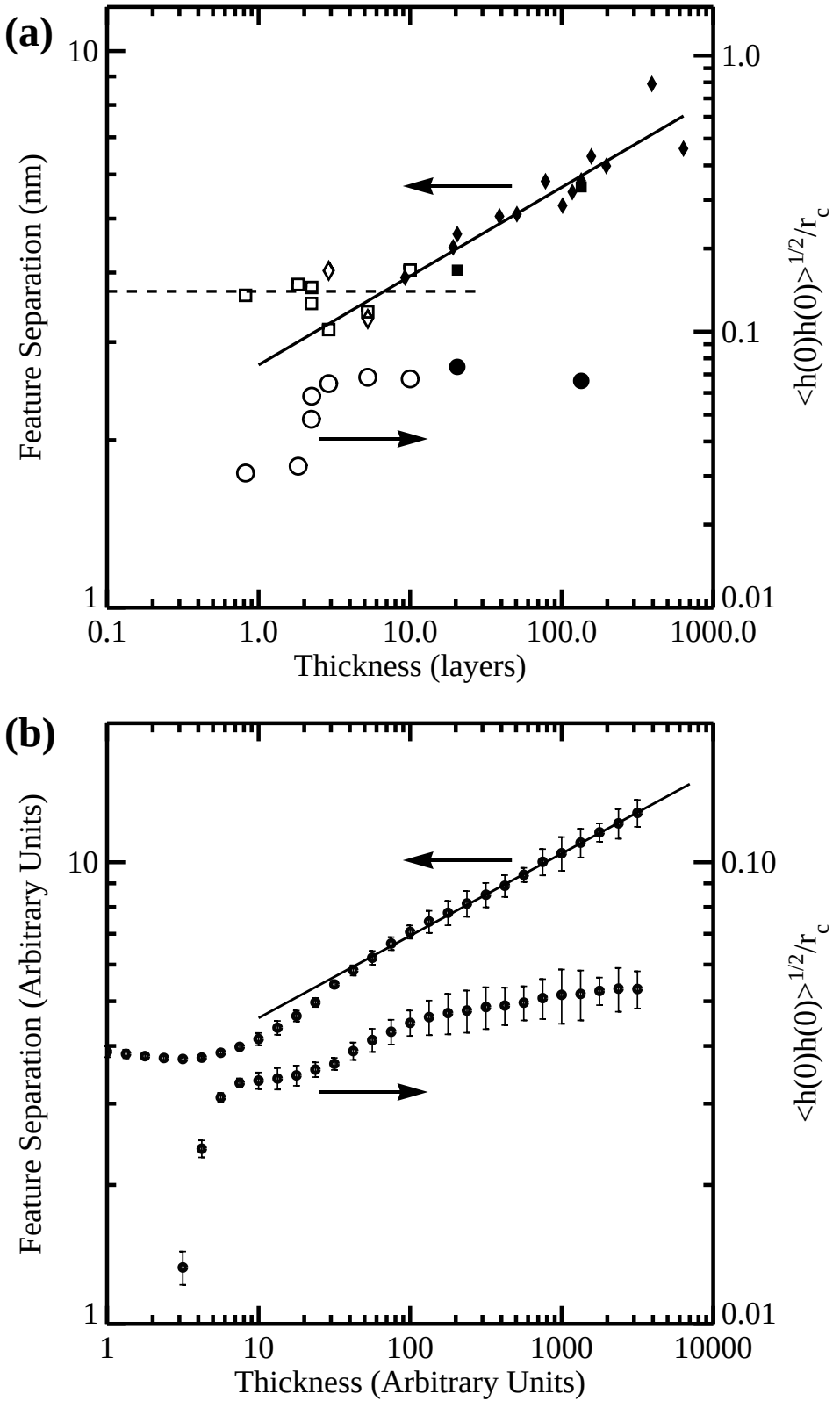
(a)
10
1
1.0
0.1
0.01
Feature Separation (nm)
<h(0)h(0)>^1/2/r_c
0.1
1.0
10.0
100.0
1000.0
Thickness (layers)
(b)
10
1
0.10
0.01
Feature Separation (Arbitrary Units)
<h(0)h(0)>^1/2/r_c
1
10
100
1000
10000
Thickness (Arbitrary Units)

Figure 3